Distance-Adaptation Wireless Power Transfer by Exploiting 2nd Harmonic Feedbacks for Implantable Medical Devices

Hao Zhang[(1)], Si-Ping Gao[(3)], Wen Wu[(2)], and Yong-Xin Guo[(3)]

(1) School of Microelectronics, Northwestern Polytechnical University, Xi'an, China
(2) Ministerial Key Laboratory of JGMT, Nanjing University of Science and Technology, Nanjing, China
(3) Department of Electrical and Computer Engineering, National University of Singapore, Singapore

Abstract

In this research, 2nd harmonics are exploited for distance-adaptation wireless power transfer (WPT). Thanks to the intrinsic discontinuity relation between 2nd harmonics and its incidence, both optimal power delivery and maximum conversion efficiency of an implantable medical device (IMD) rectifier can be tracked simultaneously by tuning the interrogated power to capture an abrupt 2nd-harmonic feedback. Harmonic-balance simulation and experimental results both validate that 2nd-harmonic feedbacks can be exploited for distance-adaptation WPT to IMDs.

1 Introduction

Wireless power transfer (WPT) for implantable medical devices (IMDs), e.g., bio-sensors and neuroprostheses [1-3] have been developed rapidly, which improves human body healthcare and therapies. However, it is difficult to realize distance-adaptation WPT to an IMD that is deeply embedded in tissues constrained by dynamic environment [4, 5]. Usually, it requires a method rely on acquisitions of wireless feedbacks to compensate for some environmental variations from physiological motions, devices migrations. Some of current methods, however, are constrained by the circuit complexities added to the IMDs and lack of direct wireless power control [6-8].

Recently, a WPT control by 2nd-harmonic feedback to an IMD was demonstrated according to an abrupt change of backscattered 2nd-harmonic signals from diode's inherent threshold nonlinearity [9]. It enables a direct measure of power levels extracted by the IMD rectifier, and requires no added circuit modification. However, the effect of 2nd-harmonic discontinuity occurs at its threshold voltage (i.e., ultralow power), which generates too low 2nd harmonic to satisfy a link budget through high-loss human tissues [10-13]. Hence, another 2nd-harmonic discontinuity of an IMD is exploited to guarantee a mitigation of penetration loss through human tissue for more practicality in this research. As shown in Fig. 1, due to the intrinsic nonlinearity of an IMD rectifier, 2nd-harmonic power can be generated when fundamental-frequency (ω_0) signal is interrogated. Since 2nd harmonic has a similar relation with its incidence ($P_{\omega 0}$) compared to the direct current (dc) [i.e., power conversion efficiency (η) inserted by a blue dash box in Fig. 1], it can

be feedbacked by a dual-band antenna and a directional coupler, then sensed by a signal analyzer for a distance-adaptation WPT (i.e., tracking both $P_{optimal}$ and η_{max} with various distances) to IMDs when an abrupt change from the backscattered 2nd harmonics occurs.
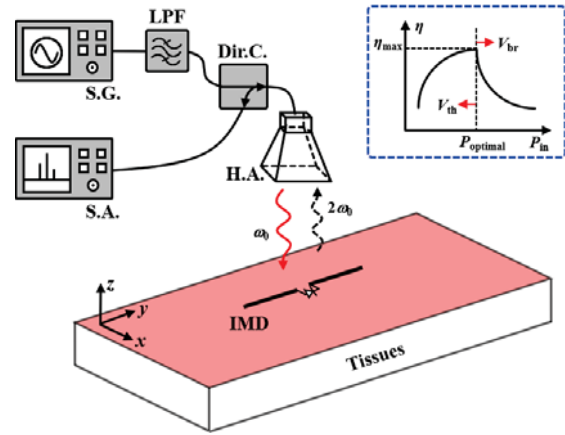
Figure 1. The proposed distance-adaptation WPT system for an IMD (S.G.: signal generator; S.A.: signal analyzer; LPF: low pass filter; Dir.C.: directional coupler; H.A.: horn antenna). Blue dash box shows the power conversion efficiency (η) versus its incidence ($P_{\omega 0}$).

2 Operation Mechanism

To validate the feasibility of proposed distance-adaptation WPT to IMDs in Fig. 1, a critical part (i.e., IMD rectifier) of an IMD is analyzed. As shown in Fig. 1, the forward (ω_0) and the backscattered ($2\omega_0$) signal channels maintain isolated from the incidence by a signal generator, whose penetration loss can be numerically calculated by considering experimental cable insertion loss and antenna radiation gains. Therefore, 2nd-harmonic feedback sensed by a signal analyzer only reveals extracted power levels of IMDs. By tuning the interrogated power from the signal generator, the distance-adaptation WPT can be attained by capturing an abrupt change of 2nd-harmonic feedbacks in signal analyzer. Followings are detailed theory analysis: *A. 2nd-Harmonic Generation*; *B. Distance-Adaptation WPT by Exploiting 2nd Harmonics.*

A. 2nd-Harmonic Generation

We assume the conversion loss of 2nd harmonic ζ, forward (ω_0) and backscattered ($2\omega_0$) free space path loss between the dual-band horn antenna (radiation gains: g_{ω_0} & $g_{2\omega_0}$) and IMD χ_{ω_0}, $\chi_{2\omega_0}$, which are strongly distance-dependent parameters. In subsequence, the 2nd-harmonic power ($P_{2\omega_0}$) sensed by signal generator can be calculated with the LPF insertion loss of γ_{LPF}, Dir.C. insertion loss of $\gamma_{Dir.C}$ and fundamental incidence (P_{ω_0}).

$$P_{2\omega_0} = P_{\omega_0}\gamma_{LPF}\gamma_{Dir.C.}g_{\omega_0}\chi_{\omega_0}\zeta\chi_{2\omega_0}g_{2\omega_0} \qquad (1)$$

Only the 2nd-harmonic conversion loss ζ varies with its incident power of P_{ω_0} when the distance between TX\RX antennas varies, and determines 2nd-harmonic generations. When derivatizing of $P_{2\omega_0}$ with respect to P_{ω_0} in (2), an abrupt change can be achieved under various distance for $P_{optimal}$ and η_{max}, i.e., distance-adaptation WPT for IMDs.

$$\frac{\partial P_{2\omega_0}}{\partial P_{\omega_0}} = k(\zeta + P_{\omega_0}\frac{\partial \zeta}{\partial P_{\omega_0}}) \qquad (2)$$

where $k = \gamma_{LPF}\gamma_{Dir.C.}g_{\omega_0}\chi_{\omega_0}\chi_{2\omega_0}g_{2\omega_0}$ is constant independent of P_{ω_0}, and the conversion loss ζ determines 2nd-harmonic abrupt change versus its incidence of P_{ω_0}.

B. Distance-Adaptation WPT by Exploiting 2nd Harmonics

As illustrated by the inserted blue dash box in Fig. 1, the power conversion efficiency (η) is typically calculated with

$$\eta = \frac{V_{dc}^2/R_L}{P_{\omega_0}} \qquad (3)$$

where V_{dc} is output dc voltage on the load resistance R_L of an IMD rectifier. As illustrated in Fig. 1, η increases with its incidence of P_{ω_0} by surpassing the diode intrinsic low threshold voltage (V_{th}). The corresponding output V_{dc} therefore increases monotonically with its incident power of P_{ω_0}. When P_{ω_0} increases high enough with its induced voltage (V_s) swinging over the diode's breakdown voltage (V_{br}), η decreases sharply, and V_{dc} is clapped to half of V_{br}. Therefore, a discontinuity of V_{dc} occurs where both $P_{optimal}$ and η_{max} can be achieved concurrently. Typically, 2nd harmonic is generated together with V_{dc}. By capturing 2nd-harmonic feedbacks in the signal analyzer, the optimal power delivery can be controlled (i.e., $P_{optimal}$ and η_{max}) when tuning interrogation of signal generator. We assume an incident signal for the IMD rectifier is $V_s\cos\omega_0 t$, whose output responses [14] can be typically expressed by

$$V_o = x_0 + x_1 V_s\cos\omega_0 t + x_2 V_s^2\cos^2\omega_0 t + \cdots \qquad (4)$$

It can be observed that only term of $x_2 V_s^2\cos^2\omega_0 t$ contributes to V_{dc} and 2nd harmonics. Therefore, similar

discontinuity of V_{dc} and $P_{2\omega_0}$ is validated, which can be exploited for a distance-adaptation WPT to IMDs. By tuning incidence (V_s) for an IMD, an abrupt change of the backscattered 2nd harmonics can be captured when it swings over V_{br}. Consequently, the distance-adaptation WPT by exploiting 2nd harmonics can be realized for IMDs.
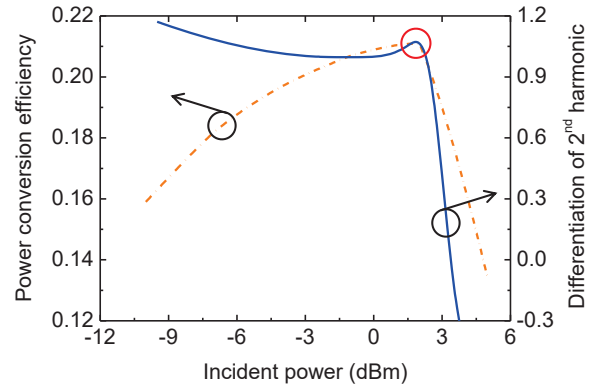
3 Experimental Validation

As illustrated in Fig. 2, a lumped rectifier is adopted for a miniaturized IMD. To ensure maximum power incidence for low-threshold diode (D_1: SMS7630) rectification, L_m and C_m are used for matching network. A dc pass filter of C_L and R_L are introduced to output a stable V_{dc} on R_L. Additionally, 25-mil high-dielectric ($\varepsilon_r = 11.2$) substrate RO3010 is utilized for further IMD miniaturization.
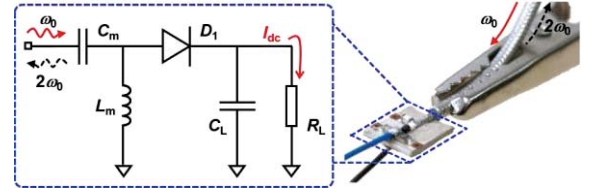
Figure 2. Schematic of a lumped IMD rectifier with insert of its PCB realization.

During experimental validations, a 50-Ω testing cable is used as a representative of IMD antenna. A directional coupler (CPL-5214-10-SMA-79, 10 dB, Midwest Microwave) is introduced to isolate the forward fundamental incidence and the backscattered 2nd-harmonic feedback, which ensures a precise measurement of power levels extracted by IMD rectifier. In further work, a dual-band antenna can be implemented for more practicality as shown in Fig. 1.

Figure 3. Experimental result of the power conversion efficiency and differentiation of 2nd harmonic. ($P_{optimal}$ and η_{max} are marked with a red circle).

The experimental result of the power conversion efficiency and differentiation of 2nd harmonic is provided

in Fig. 3. It can be observed that the 2nd-harmonic variation is smooth when the fundamental incidence ($P_{\omega 0}$) is low (~-10 to 2 dBm). In addition, 2nd harmonic increases with an increase of $P_{\omega 0}$, and undergoes an abrupt change marked with a red circle when both $P_{optimal}$ and η_{max} simultaneously occurs. Since dc power generation together with 2nd harmonics are sufficient, it will satisfy the backscattered 2nd-harmonic link budget for signal analyzer to overcome environment noise floor. Accordingly, an optimal wireless power delivery can be aided by sensing discontinue 2nd harmonics for IMDs.

4 Conclusion

2nd harmonics are exploited for distance-adaptation WPT for IMDs. Due to the discontinue 2nd harmonic ($P_{2\omega 0}$) with its interrogated power ($P_{\omega 0}$), an optimal power delivery ($P_{optimal}$) and maximum conversion efficiency (η_{max}) can be tracked simultaneously by tuning the $P_{\omega 0}$ to sense an abrupt 2nd-harmonic change. Experimental result validates that the discontinue 2nd-harmonic feedbacks have a close correspondence to both $P_{optimal}$ and η_{max}, which can be further exploited by integrating a dual-band antenna to directly control an optimal power delivery to an IMD deeply implanted into the human tissues, which brings a high insight for precise biomedical applications.

5 Acknowledgements

6 References

1. A. K. RamRakhyani, S. Mirabbasi and M. Chiao, "Design and Optimization of Resonance-Based Efficient Wireless Power Delivery Systems for Biomedical Implants," in *IEEE Transactions on Biomedical Circuits and Systems*, vol. 5, no. 1, pp. 48-63, Feb. 2011.

2. A. P. Chandrakasan, N. Verma, and D. C. Daly, "Ultralow-power electronics for biomedical applications," in *Annual Review of Biomedical Engineering*, vol. 10, pp. 247-274, 2008.

3. A. Bansal, F. Yang, T. Xi, Y. Zhang, and J. S. Ho, "In vivo wireless photonic photodynamic therapy," in *Proceedings of the National Academy of Sciences of the United States of America*, vol. 115, no. 7, pp. 1469-1474, Jan. 2018.

4. P. R. Troyk and M. A. K. Schwan, "Closed-loop class E transcutaneous power and data link for MicroImplants," in *IEEE Transactions on Biomedical Engineering*, vol. 39, no. 6, pp. 589-599, June 1992.

5. P. Si, A. P. Hu, S. Malpas and D. Budgett, "A Frequency Control Method for Regulating Wireless Power to Implantable Devices," in *IEEE Transactions on Biomedical Circuits and Systems*, vol. 2, no. 1, pp. 22-29, March 2008.

6. P. Cong, N. Chaimanonart, W. H. Ko and D. J. Young, "A Wireless and Batteryless 10-Bit Implantable Blood Pressure Sensing Microsystem with Adaptive RF Powering for Real-Time Laboratory Mice Monitoring," in *IEEE Journal of Solid-State Circuits*, vol. 44, no. 12, pp. 3631-3644, Dec. 2009.

7. M. Kiani and M. Ghovanloo, "An RFID-Based Closed-Loop Wireless Power Transmission System for Biomedical Applications," in *IEEE Transactions on Circuits and Systems II: Express Briefs*, vol. 57, no. 4, pp. 260-264, April 2010.

8. D. Ahn and S. Hong, "Wireless Power Transmission with Self-Regulated Output Voltage for Biomedical Implant," in *IEEE Transactions on Industrial Electronics*, vol. 61, no. 5, pp. 2225-2235, May 2014.

9. Xi Tian, Pui Mun Lee and John S. Ho, "Control of wireless power transfer to a bioelectronic device by harmonic feedback," in *AIP Advances*, vol. 8, no. 9, pp. 2518-3226, Aug 2018.

10. H. Zhang, S. Gao, T. Ngo, W. Wu and Y. Guo, "Wireless Power Transfer Antenna Alignment Using Intermodulation for Two-Tone Powered Implantable Medical Devices," in *IEEE Transactions on Microwave Theory and Techniques*, vol. 67, no. 5, pp. 1708-1716, May 2019.

11. Z. Bao, Y. Guo and R. Mittra, "Conformal Capsule Antenna with Reconfigurable Radiation Pattern for Robust Communications," in *IEEE Transactions on Antennas and Propagation*, vol. 66, no. 7, pp. 3354-3365, July 2018.

13. Z. Bao, "Comparative Study of Dual-Polarized and Circularly-Polarized Antennas at 2.45 GHz for Ingestible Capsules," in *IEEE Transactions on Antennas and Propagation*, vol. 67, no. 3, pp. 1488-1500, March 2019.

14. H. Zhang, Y. Guo, S. Gao and W. Wu, "Wireless Power Transfer Antenna Alignment Using Third Harmonic," in *IEEE Microwave and Wireless Components Letters*, vol. 28, no. 6, pp. 536-538, June 2018.